Scaling of the resistance in the two-dimensional Anderson tight-binding model for disordered systems

1992 J. Phys.: Condens. Matter 4 7865

(http://iopscience.iop.org/0953-8984/4/39/002)

J. Phys.: Condens. Matter 4 (1992) 7865–7876. Printed in the UK

Scaling of the resistance in the two-dimensional Anderson tight-binding model for disordered systems

Indra Dasgupta, Tanusri Saha and Abhijit Mookerjee

S N Bose National Centre for Basic Sciences, DB 17, Sector 1, Salt Lake City, Calcutta 700064, India

Received 17 October 1991, in final form 10 March 1992

Abstract. We combine the ideas of real-space renormalization and the vector recursion technique for multilead scattering to study the scaling of resistance with size for a disordered square lattice. We obtain an indication of predominant power-law dependence of the logarithm of the averaged resistance with size in the intermediate disordered regime, which smoothly changes to logarithmic behaviour as the disorder goes to zero.

1. Introduction

The aim of this paper is to combine the ideas of the vector recursion technique (Godin and Haydock 1988, Basu *et al* 1991) and real-space renormalization to study the scaling of resistance in disordered two-dimensional systems. Two-dimensional systems have been studied earlier. McKinnon and Kramer (1981) have used a slice recursion technique to estimate the behaviour of the localization length. They claim that for two-dimensional systems (even for small disorders) they find no evidence of anything other than exponential localization. However, in a later communication, Kramer (1988) states that this result (exponential localization) holds asymptotically and says nothing about power-law localized states in an intermediate regime as reported by Schreiber (1985). Power-law or weak localization was reported by Picard and Sarma (1981); however, their system sizes were rather small and their conclusions have been criticized on this point (McKinnon and Kramer 1981). Pastawski *et al* (1983) have used the convergence of a matrix recursion expansion of the Green function to examine the behaviour of the localization length. They find that as the width of the slices increases, a significant proportion of the localized states (for different configurations) shows non-exponential localization.

If we carefully analyse the basic assumptions underlying the slice recursions, we come across several points which perhaps need further discussion.

The first point is that, in order that the relation between the Green function and localization length should hold, the lengths of the slices have to be very large. McKinnon and Kramer take slices of length 30000, while Pastawski *et al* must have also taken similar lengths, but their convergence presumably occurred for far fewer steps. On the other hand the maximum widths reached for two dimensions was around 32. The extrapolation to larger widths was achieved by noting that the localization length obeys a specific scaling law. Our work with the vector recursion technique

0953-8984/92/397865+12$04.50

indicated that, as far as the scaling behaviour of the transmittance goes, a truly one-dimensional chain and a very narrow two-dimensional strip behave in similar manners, but rather differently from a square or rectangular block. It seems, therefore, rather suspect to assert that the scaling behaviour of a very narrow strip will extrapolate to large square or rectangular systems. There could be a crossover in behaviour as we increase the width of the strip. The work of Pastawski *et al* seems to indicate that this is true. As the width increases, the proportion of non-exponentially localized states increases. This is clearly evident for the lower disorders (for $W = 4$, the proportion becomes unity at a width of around 12). The same trend is evident for higher disorders, and their numerical graph indicates that, even for high disorders, the proportion definitely increases with increasing width and, had they achieved large enough widths (compared with the lengths of 30 000!), the onset of non-exponential localization would have been demonstrated.

The second point refers to the stability of the slice recursion itself, which prevents one from accurately going to large widths. Within the slice recursions the Green function or the transfer matrices contain ratios of polynomials whose orders are comparable with the number of basis states. In slice recursion, the Green function for an isolated but large slice is a sensitive function of E with zeros and poles close to the real energy axis. In the slice recursion, many numbers of greatly differing magnitudes are added together, and the errors accumulate much more rapidly than with the vector recursion technique, whose three-term recurrences involve the addition of few numbers of roughly equal magnitudes. This relative stability of the vector recursion has been discussed in detail by Godin and Haydock (1988).

Finally, since our aim is to study large square or rectangular blocks, we shall combine vector recursion with a real-space renormalization technique. This will enable us to extend our study to effectively very large sizes, although our actual calculations will be limited to relatively small blocks. However, at every step of the renormalization we shall maintain the square or rectangular shape and never resort to strip geometry.

2. Formalism

2.1. Multilead vector recursion

Our system is a two-dimensional lattice with $2N$ sites. The Hamiltonian has disorder in the diagonal terms. We attach $2M$ perfectly ordered semi-infinite leads covering its boundaries. M of these are incoming leads and M are outgoing leads. In essence there is no distinction between incoming and outgoing leads. Later in our formulation we shall remove this distinction. The purpose of these leads is to bear the incoming, reflected and transmitted waves into and away from the sample. We shall simulate the system and the leads by the following tight-binding nearest-neighbour Hamiltonian:

$$H_{\text{sample}} = \sum_{m=1}^{2N} \epsilon_m |m\rangle\langle m| + \sum_{\{m\ n\}} \sum V |m\rangle\langle n| \tag{1a}$$

$$H_{\text{leads}} = V_L \sum_{\{m'\ n'\}} \sum |m'\rangle\langle n'|. \tag{1b}$$

The tight-binding basis $\{|m\rangle\}$ spans the sample while $\{|m'\rangle\}$ spans the leads. The off-diagonal terms V of the sample are chosen to be unity. This sets the scale

of energy. The off-diagonal terms V_L in the leads determine the energy window of the incoming and outgoing electrons and are chosen accordingly. The diagonal terms in the lead Hamiltonian are taken to be zero, setting the zero of the energy. The diagonal terms in the sample are uniformly and randomly distributed in the range $-W/2 < \epsilon_m < W/2$, so that

$$\mathcal{P}(\epsilon) = \begin{cases} 1/W & \text{for } -W/2 < \epsilon < W/2 \\ 0 & \text{otherwise.} \end{cases} \tag{2}$$

The solution of the Schrödinger equation in the leads are travelling Bloch waves of the form

$$\Psi_L = \sum_m A \exp(\pm i m\vartheta)|m\rangle. \tag{3}$$

As the wave travels in the leads, the phase of its wavefunction changes by ϑ, where

$$\cos\vartheta = E/2V_L \tag{4}$$

E being the energy of the incoming electron. Note that, in order to have propagating solutions, $|E| < 2V_L$. This sets the energy window.

When the electronic wave enters the system from the leads, it is scattered. Part of it is reflected into the M incoming leads and part of it is transmitted into the M outgoing leads. Let us denote the reflection coefficient of the wavelet coming in from the ith incoming lead and reflected into the jth incoming lead by $r_{ij}(E)$, and the transmission coefficient of the same wavelet transmitted into the j'th outgoing lead as $t_{ij'}(E)$.

To obtain the transmittance and reflectance we first block tridiagonalize the Hamiltonian using the vector recursion technique (Godin and Haydock 1988, Basu *et al* 1991). This involves changing to a new vector basis. A representation of the original basis $|m\rangle$ consists of column vectors of length $2N$. A representation of the new vector basis consists of matrices of size $2N \times 2M$. The members of the new basis are generated in the following way.

The first member of the basis is chosen to be

$$|\Phi_1\} = (|i_1\rangle|i_2\rangle \ldots |i_M\rangle|o_1\rangle|o_2\rangle \ldots |o_M\rangle) \tag{5a}$$

where $|i_k\rangle$ and $|o_k\rangle$ are the positions at which the incoming and outgoing leads attach to the system.

The subsequent members of the basis are generated from

$$\begin{aligned} \mathbf{B}_1^\dagger|\Phi_1\} &= (\mathbf{H} - \mathbf{A}_0)|\Phi_0\} \\ \mathbf{B}_{n+1}^\dagger|\Phi_{n+1}\} &= (\mathbf{H} - \mathbf{A}_n)|\Phi_n\} - \mathbf{B}_n|\Phi_{n-1}\} \qquad \text{for } n > 0. \end{aligned} \tag{5b}$$

The matrix inner product is defined as

$$\{\Phi|\Psi\}^{\mu\nu} = \sum_{i=1}^{M} \Phi_i^\mu \Psi_i^\nu \qquad \text{and orthogonality as } \{\Phi|\Psi\} = \mathbf{I}.$$

It can easily be shown that the $2M \times 2M$ matrices $\mathbf{A}_n$ and $\mathbf{B}_n$ are the block-tridiagonal members of the matrix representation of the Hamiltonian in the new basis:

$$\begin{aligned} \mathbf{A}_n &= \{\Phi_n|\mathbf{H}|\Phi_n\} \\ \mathbf{B}_n &= \{\Phi_{n+1}|\mathbf{H}|\Phi_n\}. \end{aligned} \tag{6}$$

The wavefunction $|\Psi\}$ may be represented in this new basis by a set $\{\psi_n\}$ so that $|\Psi\} = \sum_n \psi_n|\Phi_n\}$. These wavefunction amplitudes ψ_n also satisfy an equation identical with (5*b*).

The boundary conditions may be imposed from the known solution in the leads:

$$\psi_0 = \begin{pmatrix} 1 + r_{11} + r_{12} + \ldots + r_{1M} \\ 1 + r_{21} + r_{22} + \ldots + r_{2M} \\ \ldots \quad \ldots \quad \ldots \\ t_{M+1,1} + t_{M+1,2} + \ldots + t_{M+1,M} \\ \ldots \quad \ldots \quad \ldots \\ t_{2M,1} + t_{2M,2} + \ldots + t_{2M,M} \end{pmatrix} \tag{7}$$

$$\psi_1 = \begin{pmatrix} \exp(\mathrm{i}\vartheta) + r_{11}\exp(-\mathrm{i}\vartheta) + r_{12}\exp(-\mathrm{i}\vartheta) + \ldots + r_{1M}\exp(-\mathrm{i}\vartheta) \\ \exp(\mathrm{i}\vartheta) + r_{21}\exp(-\mathrm{i}\vartheta) + r_{22}\exp(-\mathrm{i}\vartheta) + \ldots + r_{2M}\exp(-\mathrm{i}\vartheta) \\ \ldots \quad \ldots \quad \ldots \quad \ldots \\ t_{2M,1}\exp(-\mathrm{i}\vartheta) + t_{2M,2}\exp(-\mathrm{i}\vartheta) + \ldots + t_{2M,M}\exp(-\mathrm{i}\vartheta) \end{pmatrix}.$$

The amplitude at the nth basis ψ_n may be written as

$$\psi_n = \mathbf{X}_n\psi_0 + \mathbf{Y}_n\psi_1 \tag{8}$$

where $\mathbf{X}_n$ and $\mathbf{Y}_n$ satisfy the same recurrence relation as (5) with $E\mathbf{I}$ replacing $\mathbf{H}$ and also satisfy the boundary conditions $\mathbf{X}_0 = \mathbf{I}$ and $\mathbf{X}_1 = \mathbf{0}$, while $\mathbf{Y}_0 = \mathbf{0}$ and $\mathbf{Y}_1 = \mathbf{I}$. Note that $\mathbf{X}$ and $\mathbf{Y}$ are $2M \times 2M$ matrices.

This new basis terminates after $\nu = 2N/2M$ steps, as the rank of the space spanned by the original tight-binding basis remains unchanged after the transformation. Hence the recursion also terminates after ν steps. This gives an additional boundary condition

$$\mathbf{X}_{\nu+1}\psi_0 + \mathbf{Y}_{\nu+1}\psi_1 = 0. \tag{9}$$

If we now interchange the incoming and outgoing leads, we obtain another set of reflection coefficients r'_{ij} and transmission coefficients t'_{ij}. We may put these together in the scattering $\mathbf{S}$-matrix as

$$\mathbf{S} = \begin{pmatrix} r_{11}\ r_{12}\ \ldots\ r_{1M}\ t'_{2M,1}\ \ldots\ t'_{2M,M} \\ \ldots \quad \ldots \quad \ldots \quad \ldots \\ r_{M1}\ r_{M2}\ \ldots\ r_{MM}\ t'_{M+1,1}\ \ldots\ t'_{M+1,M} \\ t_{M+1,1}\ \ldots\ t_{M+1,M}\ r'_{M,1}\ \ldots\ r'_{MM} \\ \ldots \quad \ldots \quad \ldots \quad \ldots \\ t_{2M,1}\ \ldots\ t_{2M,M}\ r'_{11}\ \ldots\ r'_{1M} \end{pmatrix} \tag{10}$$

which may be obtained from

$$\mathbf{S} = -[\mathbf{X}_{\nu+1} + \mathbf{Y}_{\nu+1}\exp(-\mathrm{i}\vartheta)]^{-1}[\mathbf{X}_{\nu+1} + \mathbf{Y}_{\nu+1}\exp(\mathrm{i}\vartheta)]. \tag{11}$$

In the absence of magnetic fields, time-reversal symmetry holds and the two blocks containing the transmission coefficients are identical, while the terms in the blocks containing the reflection coefficients differ only in phase factors.

The reflectance into the ith incoming channel is given by

$$R_i(E) = \sum_{j \in \mathcal{I}} |r_{ij}(E)|^2 \tag{12a}$$

and similarly the transmittance into the ith outgoing channel is given by

$$T_i(E) = \sum_{j \in \mathcal{O}} |t_{ij}(E)|^2. \tag{12b}$$

Here $\mathcal{I}$ and $\mathcal{O}$ denote the sets of incoming and outgoing leads (Imry 1986). The Landauer formula then gives the zero-temperature conductance as

$$g = \frac{1}{\rho} = \frac{e^2\pi}{\hbar}\left[\left(\sum_i T_i(E)\sum_i \frac{1}{v_i}\right)\Big/\sum_i R_i(E)\frac{1}{v_i}\right]\Bigg|_{E=\mu}$$

where v_i is the velocity of the electrons carrying current in the ith channel and μ is the chemical potential of the system. In our case all the channels are equivalent, so that $v_i = v_F$, the Fermi velocity of the system. The above equation reduces to

$$g = 1/\rho = (e^2\pi/\hbar)MT(\mu)/R(\mu) \tag{12c}$$

where M is the number of incoming and outgoing channels, and $T(E) = \sum_i T_i(E)$ and $R(E) = \sum_i R_i(E)$ are the total transmittance and reflectance with $T(E) + R(E) = M$.

2.2. *Real-space renormalization*

The renormalization procedure that we shall follow closely resembles the idea of block spins in the magnetic problem. We shall divide the two-dimensional square lattice into rectangular blocks $M_1 \times M_2$ in size as shown in figure 1(*a*). We may now look at an isolated block as in figure 1(*b*). The bonds which attach it to the rest of the system now appear as input and output leads into the block. These input leads bring in an electronic wave from the rest of the system into the block. The block then scatters this wave, the output leads take the wave away from the block and it re-enters back into the rest of the system. The vector recursion technique now enables us to obtain the scattering S-matrix which describes the scattering characteristics of this block in terms of its reflectance, transmittance or resistance. Note that these three properties are not independent. The transmittance and reflectance are related by the sum rule $R(E) + T(E) = M$, since there is no inelastic scattering and energy is conserved. The resistance is the ratio of these two.

The crucial step is to obtain an *equivalent single-site scatter of the same resistance* as the block. This single-scattering site is characterized by an *effective Hamiltonian with diagonal term* $\hat{\epsilon}$.

To obtain $\hat{\epsilon}$ we proceed as follows: to this effective single-site scatterer we attach two semi-infinite, perfectly conducting leads, in exact analogy to the vector recursion

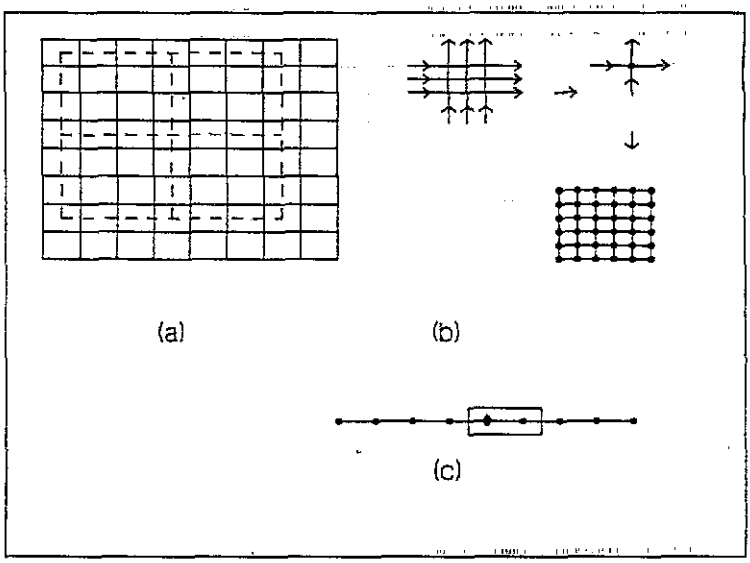

Figure 1. (*a*) Partition of the lattice into blocks. (*b*) An isolated block, renormalization of the block to a single scatterer and the renormalized lattice. (*c*) The single-site scatterer with ordered leads.

procedure described earlier (see figure 1(*c*)). In this simple problem, the vector recursion equations (5a) can be solved by hand to obtain

$$\mathbf{A}_1 = \begin{pmatrix} \hat{\epsilon} & V_L \\ V_L & 0 \end{pmatrix} \qquad \mathbf{B}_1 = \begin{pmatrix} V_L & 0 \\ 0 & V_L \end{pmatrix}$$

$$\mathbf{B}_2^\dagger \mathbf{X}_2 = \begin{pmatrix} -V_L & 0 \\ 0 & -V_L \end{pmatrix} \qquad \mathbf{B}_2^\dagger \mathbf{Y}_2 = \begin{pmatrix} E - \hat{\epsilon} & -V_L \\ -V_L & E \end{pmatrix}$$

so that the S-matrix is given by

$$\mathbf{S} = -[\mathbf{B}_2^\dagger \mathbf{X}_2 + \mathbf{B}_2^\dagger \mathbf{Y}_2 \exp(-\mathrm{i}\vartheta)]^{-1}[\mathbf{B}_2^\dagger \mathbf{X}_2 + \mathbf{B}_2^\dagger \mathbf{Y}_2 \exp(\mathrm{i}\vartheta)].$$

The various symbols have already been introduced earlier. The reflection and transmission coefficients are given by

$$r(E) = \mathbf{S}_{11} = [(E - \hat{\epsilon})V_L \exp(-\mathrm{i}\vartheta) + V_L E \exp(-\mathrm{i}\vartheta) - (E - \hat{\epsilon})E]/\Delta$$

$$t(E) = \mathbf{S}_{21} = (2\mathrm{i}V_L^2 \sin\vartheta)/\Delta$$

where

$$\Delta = \det[\mathbf{B}_2^\dagger \mathbf{X}_2 + \mathbf{B}_2^\dagger \mathbf{Y}_2 \exp(-\mathrm{i}\vartheta)].$$

Now, using the Landauer formula and equation (4) we obtain a relationship between the resistance and $\hat{\epsilon}$:

$$\rho = (e^2\pi/\hbar)|r(E)|^2/|t(E)|^2 = (e^2\pi/\hbar)\hat{\epsilon}^2/(4V_L^2 - E^2).$$

If we express the resistance in units of $e^2\pi/\hbar$, then

$$\hat{\epsilon} = \sqrt{\rho(4V_L^2 - E^2)}. \tag{13}$$

If we are interested only in the resistance as a physically observable quantity and ignore the detailed wavefunction characteristics within the sample, then these two systems, namely the block and the single scatterer, are *equivalent*. We may then replace the Hamiltonian for the block by the *effective* Hamiltonian of the single scatterer. We may do this to every block in figure 1(*a*) and finally obtain the renormalized system as in figure 1(*b*). In doing this we have replaced a system with N sites by a much smaller system of N/M_1M_2 sites.

The analogy with the block spin idea is now evident. There we replace a block of spins by a single *effective* spin and an *effective* coupling $\hat{J}_{ij}$ such that the free energy remains invariant. Here we replace a block of scatterers by a single *effective* scatterer with an *effective* diagonal Hamiltonian term $\hat{\epsilon}$, such that the resistances of the block and scatterer remain invariant:

$$\hat{H}_{\text{eff}} = \sum_I \hat{\epsilon}_I |I\rangle\langle I| + \sum_I \sum_J V |I\rangle\langle J|. \tag{14}$$

Since the different blocks involve random Hamiltonian elements, the new effective $\{\hat{\epsilon}_I\}$ are also random. The distribution of these $\hat{\epsilon}_I$ may be determined from the distribution of the block resistances.

The renormalization procedure may now be iterated, by dividing the renormalized lattice of figure 1(*b*) into blocks and reducing these by an identical procedure, obtaining a second level set $\{\hat{\epsilon}'_I\}$. This will reduce the sample to a size $N/(M_1M_2)^2$. At each stage of the renormalization procedure the vector recursion will always involve a fixed size $M_1 \times M_2$ but will give us information about systems of increasingly larger sizes.

We are, however, limited by the fact that, if all states are localized, the resistance will increase with increasing size, eventually reaching values too large for the computer to handle. Moreover, since we are interested in finding how the resistance behaves with size, unlike in the usual renormalization procedure, we cannot rescale down the resistance at each iteration step. This difficulty occurs for large disorders, even for relatively small sizes as the resistances are very large.

Our work is complementary to that of Kramer (1988). Kramer (1988) claims that his results are consistent with exponential localization only. This holds asymptotically and does not say anything about (power-law) decay of the states in the intermediate regime.

3. Results and discussion

Figure 2 shows the distribution of the diagonal Hamiltonian elements of the *effective single-site scatterers* at the end of the first four block renormalizations. Since the Hamiltonian elements of the individual blocks are random, the effective scatterer elements $\{\epsilon\}$ are themselves random. Their distribution is obtained by running the vector recursions over up to 500 configurations of the block and obtaining the distribution as histograms. This distribution is used in the next iteration to generate

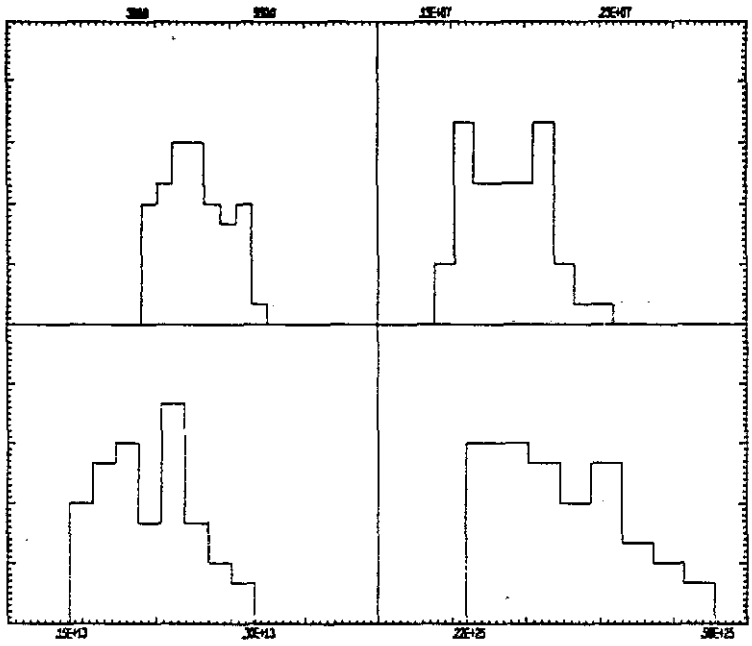

Figure 2. The distribution of scattering elements for four successive steps in the renormalization (only the positive part of the ϵ axis is shown).

the effective Hamiltonians. Several features of the distributions may be commented upon.

We have started from a uniform distribution centred at the origin. We first note that from the relationship between the resistance and ϵ for a single scatterer the sign of $\hat{\epsilon}$ is immaterial. $\hat{\epsilon}$ and $-\hat{\epsilon}$ both give the same resistance. Moreover at every step of the renormalization the distributions of $\{\hat{\epsilon}\}$ are symmetric about the origin. In figure 2 we have shown only the positive part of the $\hat{\epsilon}$ axis. It is clear that with each iteration a hole of increasing width opens up at the origin although at the starting point there was no hole at the centre of the distribution. Why is this so? The initial distribution shows that there is a finite probability that $\hat{\epsilon}$ takes a value in the neighbourhood of zero. However, after the first renormalization, $\hat{\epsilon}$ can only be zero if all $\{\epsilon\}$ of the constituent block are zero. The probability that a number of ϵ-values are simultaneously near zero is very small. This probability becomes progressively smaller as we go on iterating the renormalization procedure. Each wing of the distribution function becomes centred about values that are progressively larger. Although we have shown the results near the band centre, this is true for all values of the incoming energy within the energy window. This indicates that all states in two dimensions are localized and the resistance due to the disorder scattering is highly non-Ohmic.

For the scaling calculations we have used blocks of sizes 48, 120 and 224. Very small blocks should not be used as the effect of quantum coherence which is the basic cause of localization may not effectively be demonstrated. Very large blocks also pose problems since their resistances become too large for numerical stability. The strength of disorder is measured by the quantity $\delta = W/B$ where B is the band

width (energy window of the problem). We first study the case of a moderate disorder $\delta = 0.5$ at $E = 0.5$. Figure 3 shows the plot of $\langle \log \rho \rangle$ versus log(size). The points are numerical values. These correspond to blocks of sizes 48, 48^2, 48^4 and 48^8, 112 and 112^2, and 224 and 224^2. The figure also shows the least-squares fitted straight line, appropriate for a power-law dependence of ρ on size.

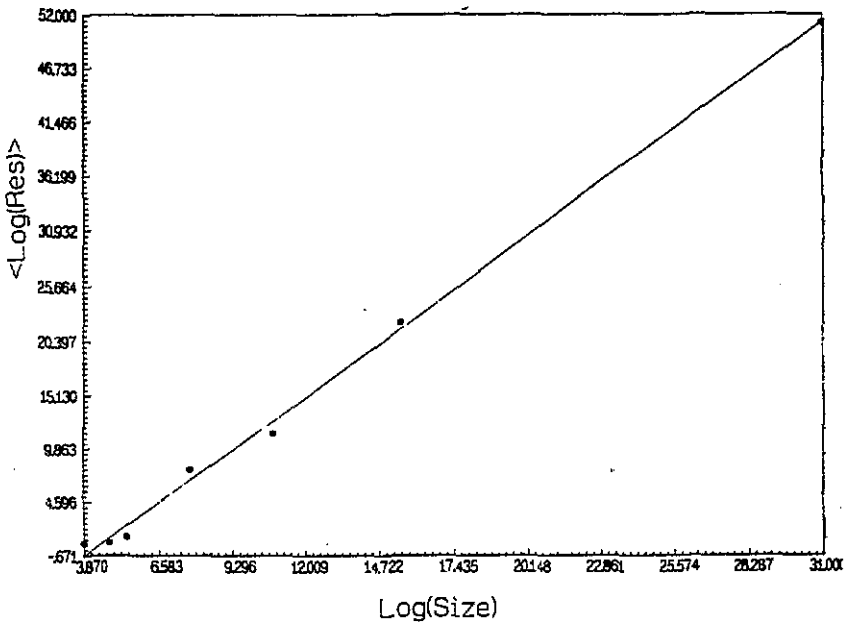

Figure 3. The averaged logarithm of the resistance versus the logarithm of the size for $E = 0.5$ and $\delta = 0.5$. (A linear fit through the data points is shown.)

Figure 4 shows a similar plot, but for disorders varying from $\delta = 6.25 \times 10^{-4}$ (for the lowest graph) to $\delta = 12.5$ (for the highest graph) at $E = 0.5$. As expected, the power α defined by $\rho(N) = \rho_0 N^{\alpha}$ is a function of the disorder parameter δ and continually decreases with increasing δ.

The above study indicates that on average the resistance scales as a power law with the size. This power decreases with the disorder strength. The curve $\delta = 0.0373\alpha^{0.529}$ is the best fit through the data points, and its extrapolation to very low disorders is shown in figure 5. In figure 6(*a*) we plot resistance versus $\log N$ for $\alpha = 1.796 \times 10^{-4}$, which corresponds to a disorder parameter $\delta = 5.0 \times 10^{-4}$. Throughout the size range quoted, the resistance variation at these low disorders is consistent with $1 + A \log N$. As a contrast in figure 6(*b*) we have shown a similar curve for $\alpha = 1$, $\delta = 0.037$, in an identical size range. Even for these disorders, the deviation from the logarithmic form is evident. For very large disorders the value of the resistance becomes so large that it becomes larger than the maximum number that our computer can handle. In conclusion it seems that power-law behaviour is the correct interpolation between exponential and logarithmic limits as predicted by single-parameter scaling theory (Abrahams *et al* 1979).

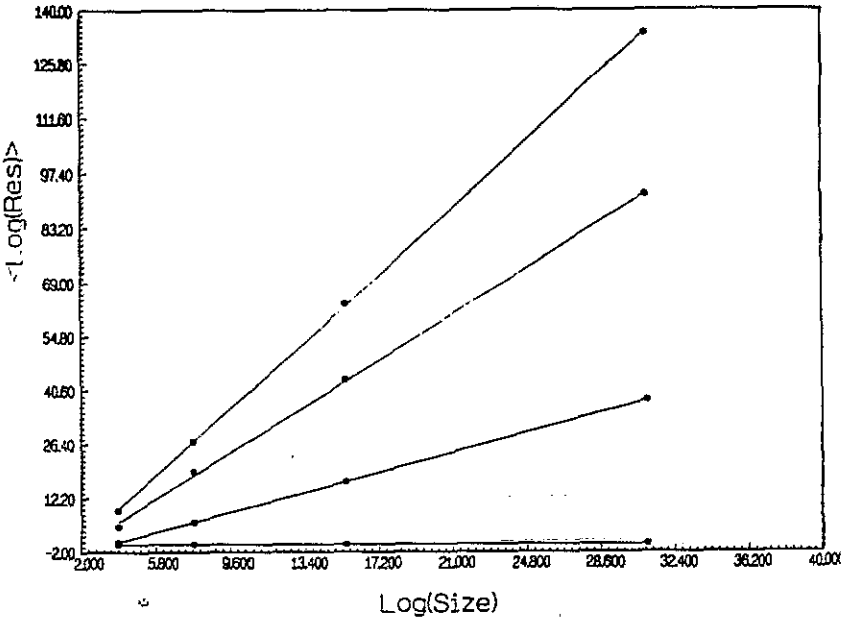

Figure 4. The averaged logarithm of the resistance versus the logarithm of the size for $E = 0.5$ and $\delta = 6.25 \times 10^{-4}$, 0.5, 5.0 and 12.5.

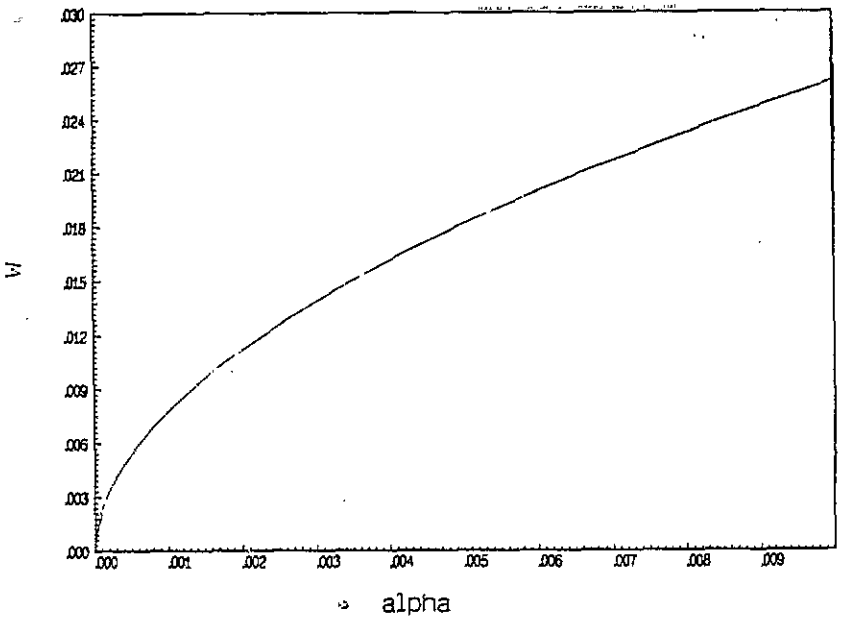

Figure 5. Variation in the width of probability distribution for $\epsilon(W)$ versus the slope α.

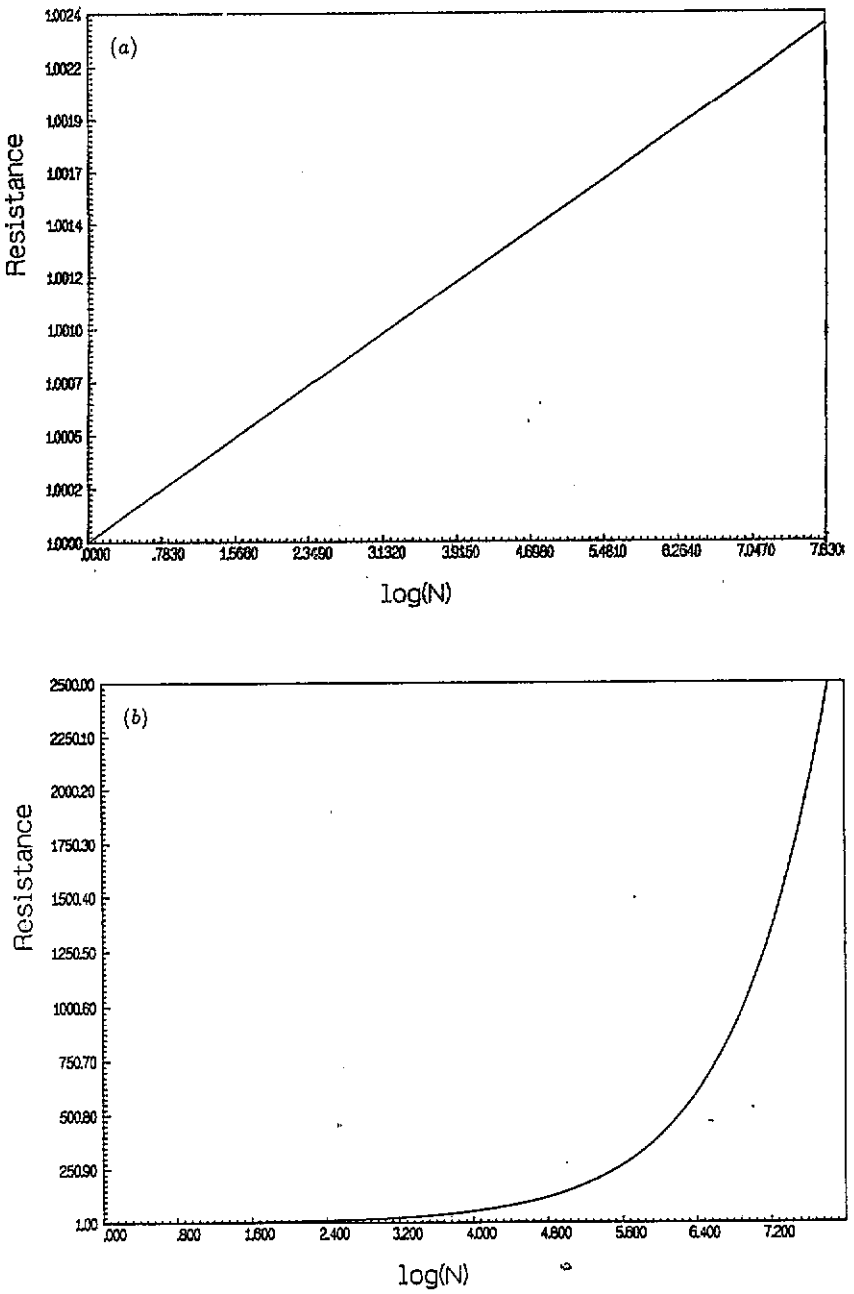

Figure 6. (*a*) Resistance versus the logarithm of the size for $\delta = 5.0 \times 10^{-4}$. (*b*) Resistance versus the logarithm of the size for $\delta = 0.037$.

Acknowledgments

The authors should like to thank the Department of Science and Technology, India, for financial support for Project SP/S2/M-56/89 under which this work has been done. We also thank C M M Nex, Cavendish Laboratory, for providing us with the vector

recursion package. AM would like to thank the International Centre for Theoretical Physics, Trieste, Italy, for hospitality whilst writing up this paper.

References

Abrahams E, Anderson P W, Licciardello D C and Ramakrishnan T V 1979 *Phys. Rev. Lett.* **42** 673
Basu C, Mookerjee A, Sen A K and Thakur P K 1991 *J. Phys.: Condens. Matter* **3** 6041
Godin T J and Haydock R 1988 *Phys. Rev.* B **38** 5237
Imry Y 1986 *Directions in Condensed Matter Physics* vol 1, ed G Grinstein and G Mazenko (Singapore: World Scientific) p 101
Kramer B 1988 *Anderson Localisation* ed T Ando and H Fukuyama (Berlin: Springer)
McKinnon A and Kramer B 1981 *Phys. Rev. Lett.* **147** 1546
Pastawski H M, Weisz J F and Albornoz S 1983 *Phys. Rev.* B **28** 6896
Picard J L and Sarma G 1981 *J. Phys. C: Solid State Phys.* **14** L127
Schreiber M 1985 *J. Phys. C: Solid State Phys.* **18** 2493